Eur. Phys. J. B (2025)98:182
https://doi.org/10.1140/epjb/s10051-025-01005-1

THE EUROPEAN PHYSICAL JOURNAL B

Regular Article - Computational Methods

Geometrical distribution of agents based on a generalised Potts model

Alejandro Rivero[1,3,a], Alfonso Tarancón[1,2], and Carlos Tarancón[3]

[1] Instituto de Biocomputación y Física de los Sistemas Complejos, Universidad de Zaragoza, Edificio I+D-Campus Río Ebro, C/ Mariano Esquillor s/n, 50018 Zaragoza, Spain
[2] Departamento de Fsica Terica, Universidad de Zaragoza, Campus San Francisco, 50009 Zaragoza, Spain
[3] Kampal Data Solutions, WTCZ, Avda. Maria Zambrano 31, 50018 Zaragoza, Spain

Received 8 March 2025 / Accepted 17 July 2025

Abstract. In collective local interaction systems with agents assigned to different profiles (categories, traits), the distribution of such profiles in the neighbourhood of any agent affects the exchange of ideas, a basic element in Collective Intelligence experiments. It is important to control this distribution experimentally, asking for criteria that should range from maximum homogeneity to maximum difference. We suggest a method where we obtain these criteria by adding an extra interaction term to the Q-state Potts model, producing a rich vacuum structure. By controlling the two parameters of the model, we can obtain different patterns for the geometrical distribution of the agents. We study the transitions and phase diagram of this model, considering the physics at constant magnetization, and show that the states correspond to a large diversity of mixing patterns, directly applicable to agent distribution in CI experiments.

1 Introduction

We are interested in the propagation of ideas in a heterogeneous environment, and to study this we have the preliminary problem of the arrangement of such an environment.

The transition between different arrangements of agents in a lattice was introduced as a subject of study in sociology by Schelling [15]. A connection to models from statistical physics [2,7,12,18] was soon noticed, particularly to the Potts model, where it is possible to consider situations with more than two profiles [2,16]. These studies were focused on segregation and aimed to find how the phase transition into clustering occurs. The social usefulness of breaking this clustering was clearly recognised not only in segregation studies but also in any deliberative process where *information bubbles* occur.

Looking at the aggregation of human agents, empirical data have corroborated the existence of different phases, ranging from echo chambers [21] to networks with strategic anti-assortativity [5], where agents' preference goes beyond simple randomisation, and they position themselves actively for contrast, avoiding homophily.

Over this structure, different models of propagation of ideas can be implemented [3] and with different network topologies [10,17,19] consensus happens in even more subtle ways, such as the enhancement of information gerrymandering [19]. Consensus itself is well known to have a phase transition depending on the probability of spreading, see [2, sect X].

We encountered the problem of agent mixing when adapting to multiple kinds of agents a platform of propagation of ideas [4] that forces consensus in a collective intelligence (CI) system. In CI we define a process where collaborations are expected to produce better ideas [9,14,22] than the aggregation of individual votes. With such decision agents, where a participant evolves from the knowledge of their neighbours, it is important not only the dissolution of the information bubble but also the knowledge of the kind of phases to which the system is driven once the clusters dissolve.

In our model, agents—usually human participants from some demographics—are located on a two-dimensional square lattice of side L with $V = L \times L$ nodes and periodic boundary conditions. In the practical implementation[1] [4] the lattice is constructed with the actual users at each moment, different from a perfect regular square, although the geometry is constructed to be as close to the square as possible. This point is not essential in this paper, and we consider square lattices thereafter, but we stress that the algorithm is expected to work with incomplete lattices. The point is that the degree of any participant in our platform is always less than or equal to four, avoiding

[a] e-mail: arivero@unizar.es (corresponding author)

[1] https://ic.kampal.com/.

Published online: 07 September 2025

some of the extra complications from network topologies referred to above.

Up to now in this CI model we have been working with experiments where all agents are humans from similar demographics, interacting in real-time in one unique process, in experiments of about one hour duration. Results from a social point of view can be seen in [13]. The motivation to use different types of agents is that now we consider the possibility of new segmented experiments, where we start with isolated experiments which after some time reunite in a single set in which all agents can interact with one another. We have different profiles, for instance, man or woman, citizens and politicians, segmentation for age or education level, etc. Segmentation can also be based on levels of agent tolerance, relevant for spatial public goods game [20]. Or even bots from AI tools can be considered to act in these collective experiments, thus providing additional profiles.

In general, we have a number $Q \geq 2$ different profiles initially evolving in their separate experiments, not dissimilar to Axelrod models [1,11], and we finally unite them in a single ensemble. At that moment, the presence of new or disruptive ideas that participants see depends on their neighbourhood.

With such multiple demographics, different options for the agent arrangement can be preferred by the experimenter; for instance, a pure random state could be preferred to a "chessboard" antiferromagnetic phase and to the assortative clustering, but also—having more than two kinds of agents – a maximally heterogeneous neighbourhood could be preferred to the one provided by randomisation and to the one provided by the AF chessboard.

Because a typical experiment in real time contains up to thousands of agents, and mixing should typically be completed in less than a minute, we need efficient tools and algorithms to construct the actual agent distribution, and the Potts-type models can address this.

To obtain all required distributions we need to introduce a second coupling, added to the standard Potts model, that tunes local heterogeneity as described in the next section. The new model presents a phase structure that supports very different geometrical agent distributions. Experimentalists can therefore tune two parameters in a continuous way to select the desired region, but the analysis in this paper simplifies their choice, as we can use the physics of the model as a guide.

2 The model

In Potts model, we consider a lattice in d dimensions, usually regular (cubic), where the variables are integer numbers, and the energy counts the number of equal neighbours. Different geometries, number of neighbours, couplings... can be considered, with different physical behaviour [6,8]. In the AF case, the dominant configurations (or vacua) tend to maximise the number of different neighbours. The main energy terms studied have been first neighbours (in $d = 2$, 4 neighbours, up, down, right and left), and second neighbours (also 4, now on diagonals). The studies consider the Macrocanonical system, where temperature T is fixed, and the q value of a node can change without restrictions, and then the global magnetizations are not fixed.

We analyse here a model with important differences with respect to previous studies.

The main difference is that we consider that the number of agents for each colour is fixed. From a sociological point of view, it is easy to understand: we must locate on a lattice for instance 4 types of agents, and we have a fixed number of each one: 23 men from cities, 17 men from rural areas, 31 women from cities, and 16 women from rural areas.

Then, we start with N total agents, with Q different types, each one with a number N_q, $q \in \{1 \dots Q\}$, the *magnetization*, where $\sum_1^Q N_q = N$. The Potts Model presents as the basic tool to mix agents while keeping a constant magnetization vector N_q. For instance in the simpler case of a $L \times L$ lattice (with even L) and $Q = 2$ if we consider very small T, the ordered phase will be two compact blocks of equal q agents. In the small T but negative coupling, the Antiferromagnetic vacuum is a chessboard pattern, with every agent surrounded entirely by different ones.

Our goal is to distribute on a two-dimensional square lattice N agents of Q types, where each type has N_q agents, with $\sum_{1,Q} N_q = N$. We define local interactions (first neighbours) to build a model (Energy or Lagrangian) that produces the desired patterns of agent mixing at a global level.

We begin by considering different possible, local-level, requirements that help us to our definition of Energy.

- R1 All neighbours q_i must have the same colour as the central node q_0
- R2 All neighbours q_i must have a different colour from the central node q_0
- R3 The central node must be surrounded by nodes with the same colour (regardless of central node colour)
- R4 The central node must be surrounded by nodes with the maximum number of different colours (regardless of central node colour)

We explain these requirements in detail.

If we consider $Q = 5$ for example, a configuration with the central node having $q = 0$ and also the four neighbours with colour $q = 0$ satisfies requirement R1. If the four neighbours are coloured with $q = 1, 1, 2, 3$, we fulfil the R2 requirement. In Fig. 1 we show the two situations.

The standard Potts model, in a square lattice, allows us to obtain these configurations, in the Ferro or Anti-

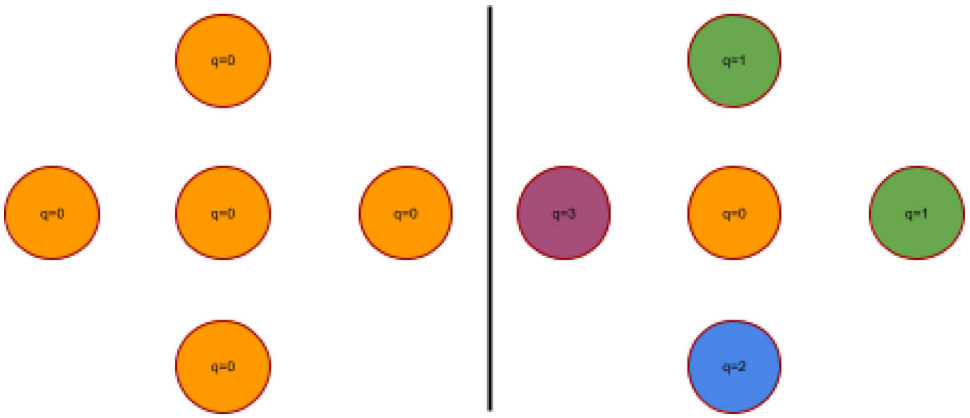

Fig. 1 Two typical configurations for $Q = 5$. The left one corresponds to requirement R1 and the right to the R2

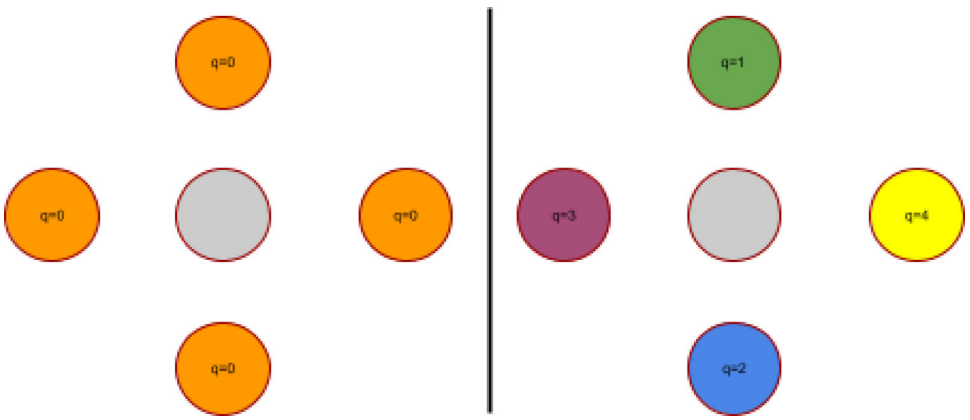

Fig. 2 Two typical configurations for $Q = 5$. The left one corresponds to requirement R3 and the right to the R4

Ferro regions. We define the standard Potts Energy as

$$\bar{E}_\kappa = \sum_{n,\mu} \delta(q(n), q(n+\mu)) \tag{1}$$

and the partition function as

$$Z = \sum_{\text{Conf}} e^{\kappa \bar{E} \kappa}$$

In the large positive κ region the system goes to Ferromagnetic vacuum, and we obtain the R1 requirement. On the contrary, if we go to large negative values of κ we obtain configurations with the R2 condition.

R3 and R4 add new conditions which indicate how many different colours we have among the neighbours of a node. In the same case with $Q = 5$ we have two opposite situations, when all neighbours are different (therefore we have 4 colours) or when all of them are the same colour. In Fig. 2 we can see both cases. It is very important to note that the colour of central node is irrelevant in this case (We will return to this point later).

However, requirements R3 and R4 must be analysed with more attention. In $d = 2$ all the possibilities can be seen in Table 1.

Table 1 Different options to define the number of different neighbours

Neighbours	Different colours	Different pairs
abcd	4	6
abcc	3	5
aacc	2	4
accc	2	3
cccc	1	0

If we want to mix agents in different ways, the *number of different colours* has the same value for *aacc* and *accc* cases. From the point of view of mixing, these two situations are different. In general, we can see that the first case is better for diversity, and then we must define a new criterion distinguishing these cases. To do that we consider *the number of different pairs* between the four neighbours. We obtain the third column in Table 1, and we break the previous degeneracy. We modify therefore R3 and R4 criteria:

- R3 The centre node is surrounded by nodes with the minimum number of different pairs (regardless of central node colour)

- R4 The centre node is surrounded by nodes with the maximum number of different pairs (regardless of central node colour)

We define $<<q_n>>$ as the set of the six pairs which can be constructed with nodes surrounding (next neighbours) the node q_n To obtain this number of pairs we define a new interaction term in the Potts model.

$$\bar{E}_\rho = \sum_{n,(a,b)\in<<q_n>>} \delta(q_a, q_b) \tag{2}$$

It is important to note that if we use only E_p the lattice is decomposed into two non-interacting sublattices (chessboard black and white). The term κ from the standard Potts is the one that couples both subnetworks. We can see E_ρ as a *plaquette* interaction in the sublattice; this is clear from Fig. 3 (right) by rotating the lattice 45 degrees.

This new term (ρ), introduced order to control *the number of different colours between first neighbours* is different from the NN usual interactions; it is a plaquette term, with two decoupled lattices, which are coupled by the standard first neighbour term (κ).

We now define the full model through the partition function

$$Z = \sum_{\text{Conf}} e^{\kappa \bar{E}_\kappa + \rho \bar{E}_\rho} \tag{3}$$

In Fig. 3 we show the interaction terms. If nodes connected by one arrow are of equal colour, their contribution to Energy is 1. On the left the standard Potts interaction (κ term). At right the new proposed pair interaction (ρ term).

3 Phase diagram

We want to study the phase diagram of our model. As previously mentioned, the system depends strongly on the choice of the M_q values. We define the Q magnetizations as

$$M_q = \sum_{n\in V} \delta(q(n), q) \tag{4}$$

To make simulations, we must fix a precise value. The structure, phases, vacua, etc. depends of course on the q and M_q distribution used. We will comment on general aspects applicable to different values of M_q and q, but for large computations on Monte Carlo, we will specifically use $q = 4$ and $M_q = V/4\ \forall q$, that is to say, we have one quarter of nodes with each colour. We maintain this ratio for the different V values.

We want to study the phase diagram in the (κ, ρ) plane. We define the observables

$$E_\kappa = (1/4V)\partial \ln Z/\partial\kappa = (1/4V)\bar{E}_\kappa$$
$$= (1/4V)\sum_{n,\mu} \delta(q(n), q(n+\mu)) \tag{5}$$
$$E_\rho = (1/6V)\partial \ln Z/\partial\kappa = (1/6V)\bar{E}_\rho$$
$$= (1/6V) \sum_{n,(a,b)\in<<q_n>>} \delta(q_a, q_b) \tag{6}$$

These energies are in the interval $[0, 1]$. To locate with precision the phase transitions, we use the associated specific heats

$$C_\kappa = \partial\langle E_\kappa\rangle/\partial\kappa = 4V(\langle E_\kappa^2\rangle - \langle E_\kappa\rangle^2) \tag{7}$$
$$C_\rho = \partial\langle E_\rho\rangle/\partial\rho = 6V(\langle E_\rho^2\rangle - \langle E_\rho\rangle^2) \tag{8}$$

These quantities can diverge at phase transitions with the Volume, according to the critical exponents; in our case, these critical exponents are not meaningful because they depend on the M_q values. Anyway, the divergence of specific heats is a clear signal of transition in the thermodynamic limit, and we will study this behaviour to locate the transition line in the phase diagram in a particular case.

We use a Monte Carlo Metropolis algorithm in a $d = 2$ square lattice with periodic boundary conditions (pbc). The elemental update takes two randomly selected sites, with different colours, and tries to interchange their colours. In this way we preserve the M_q constraints. We perform k iterations between measurements, with M measures for a block, and finally B blocks. We have therefore kMB iterations, with MB measures. To compute errors, we make blocks of size M, and we have of course B blocks. The exact values depend on L and also of the region of parameter space. We control in all cases that the system is thermalised and errors are (almost) block-size independent.

We make different runs along parameter space. First, we use a $L = 16$ lattice to explore the main properties and possible phase transitions. After that we run $L = 32$ and $L = 64$ lattices, in a smaller region around transitions, to locate transitions and to study scaling and divergences. We have runs on a grid over the space parameter, horizontals with $\rho = cte$ and verticals with $\kappa = cte$ and also along main diagonals ($\rho = \pm\kappa$). We use up to $k = 40, M = 10000, B = 100$ for each parameter values.

In Fig. 4 we plot the energies and specific heats along the vertical line $\kappa = -1, \rho \in [-2, 1]$.

After a detailed analysis the phase diagram for this case ($q = 4, M_q = V/4, \forall q$) is plotted in Fig. 5.

We have 4 different regions.

- **T0** In this region we have a disordered system, and therefore small values for Energies. This is the central part of the run in Fig. 4.
- **T1** For negative values of κ the system goes to AF situation, with each point surrounded by different colours ($E_\kappa \approx 0$), and the large value of ρ, produces that these 4 neighbours will be equal between them, with $E_\rho \approx 1$. This is possible with configurations similar to b in Fig. 6. This region corresponds

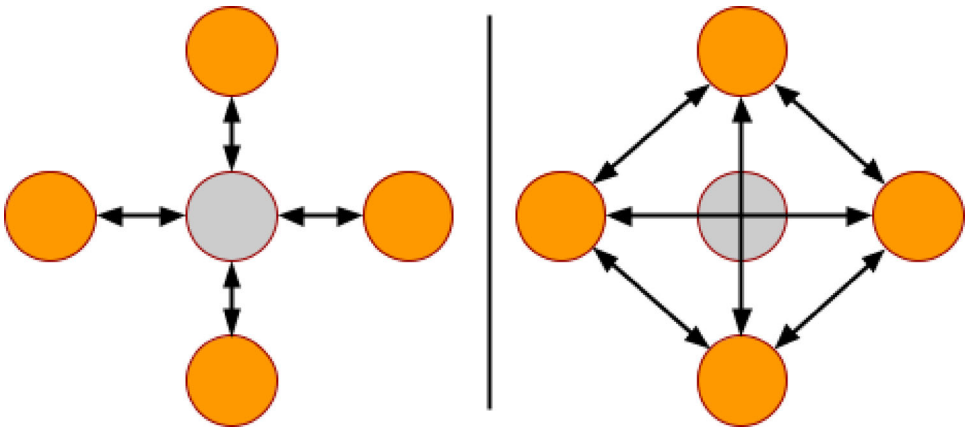

Fig. 3 Schematic representation of the 4 interactions from the κ term (left); on the right, we show the 6 terms entering the pair interaction with the ρ term

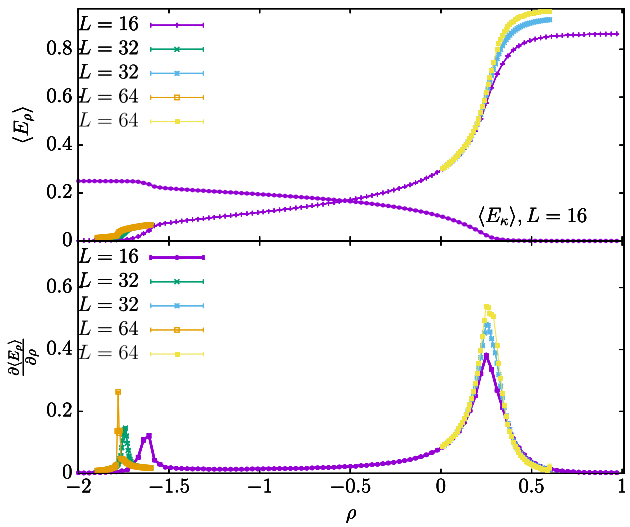

Fig. 4 Energies along the line $\kappa = -1, \rho \in [-2, 1]$

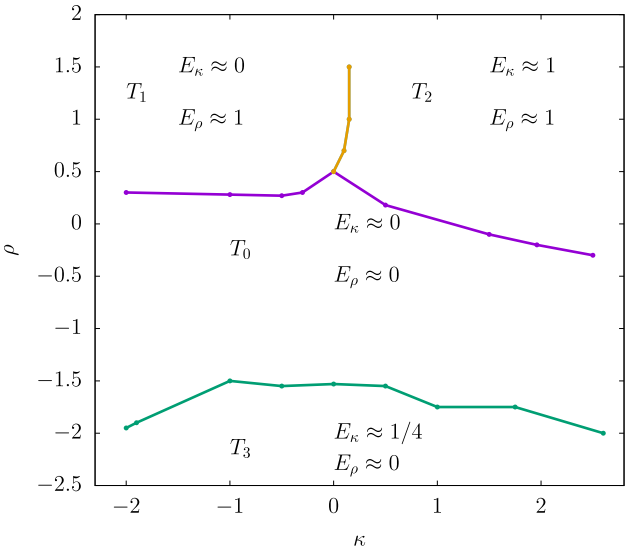

Fig. 5 Phase diagram

to positive values of ρ in Fig. 4. In this figure we have also plotted the value of $E\kappa$, to see that in this region is zero (only the $L = 16$ result is plotted)

- **T2** Here both κ, ρ are positive. Therefore the 4 neighbours tend to be equal, maximising both Energies (to their maximum value 1). Hence, we have a ferromagnetic vacuum, with the constraint of constant magnetizations. The system tends to form homogeneous blocks, like a in Fig. 6.
- **T3** Large negative values of ρ. Here E_ρ goes to zero, and we have that the 4 neighbours for each node are different. This is possible, as can be seen in c in Fig. 6. If the 4 nodes are different, one of them must be equal to the central node, and therefore $E_\kappa = 1/4$. This region corresponds to large negative values of ρ in Fig. 4. We can see that $E\rho \approx 0$, and $E_\kappa \approx 0.25$ (we plot only the $L = 16$ for this energy).

The global phase diagram has been obtained from several Monte Carlo simulations along different lines. For each possible transition, we have run $L = 16, 32, 64$ lattices, and we study the scaling of the specific heats. In Fig. 4, lower part we plot the values of C_ρ for the different sizes. In the transition from T_0 to T_1 (right peaks) we can see that the apparent critical ρ moves slightly, and the maximum value also grows up. In the T_3 to T_0 transition (around $\rho \approx -1.78$) the finite size effects are larger, with clear movement for the apparent critical ρ. The system seems to converge, and the maximum scales with L to some power (a critical exponent). All these facts point out to a phase transition in the thermodynamic limit. The transition order and critical exponents could be computed from a more in-depth finite size scaling analysis. However, this order and critical exponents depend on the details of our choice: the q and especially the M_q values. Therefore we do not consider this study here.

For these results to be of broader interest, we must consider the non magnetization-fixed model (Macrocanonical model with unconstrained magnetizations), which will be addressed in a future publication.

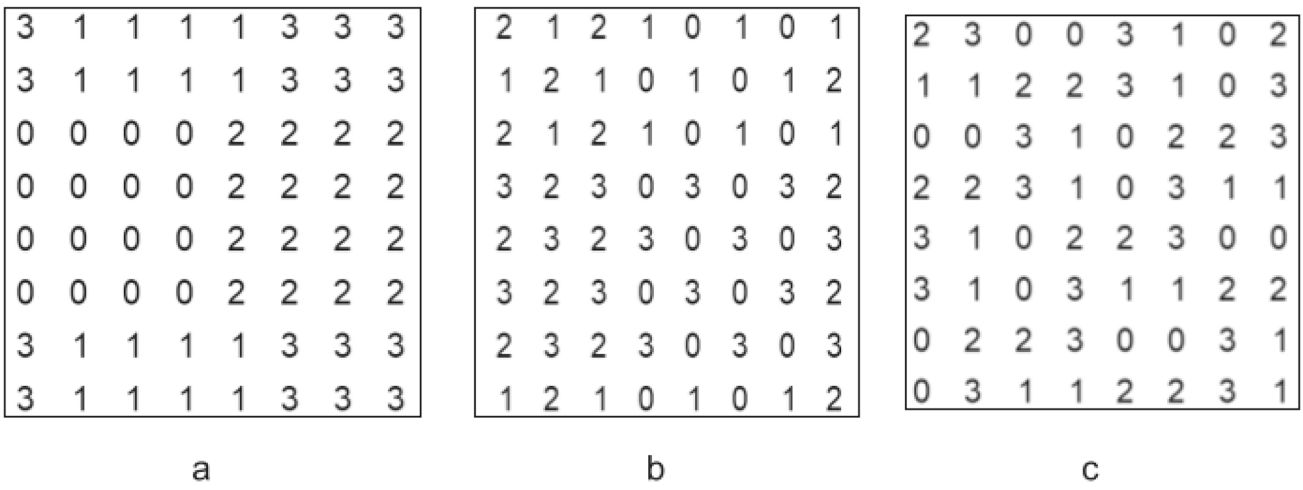

Fig. 6 Vacua examples in a $L = 8$ lattice

Based on the different runs, we have finally obtained the phase diagram of Fig. 5.

4 Experimenter selections in practice

As has been noted, the exact characteristics of the dominant configuration depend on the actual value of the parameters, corresponding to the exact position of the phase transitions and details of the phase diagram. In the implementation we usually restrict the experimenter options to a reduced number of possibilities, mainly the regions considered in previous sections, to facilitate the choice; we list in Table 2 the values of the parameters to choose for these cases.

5 Some particular cases

The introduction of this model permits us to obtain configurations with required constraints and to see if it is possible to avoid frustration and also to find different realisations or equivalent configurations. Let us consider the case $Q = 2, L = 8, N_0 = N_1 = 32$, and we want to be in a region with maximum diversity. For these values of Q and M_q we do not know the phase diagram, but we expect that in the region of $\rho \ll 0, \kappa \lesssim 0$, we will have a vacuum similar to that of the region $T3$ considered previously. (different neighbours and different pairs) In this case, the line configuration (one row with all zeros, another with all ones, etc.) optimally satisfies the constraint of having the maximum number of differences to the first neighbours, and of having the maximum number of differences between neighbours, two in each case. However, many non-homogeneous configurations satisfy exactly the same constraint, for example, a typical one obtained in the simulation and shown on the left of Fig. 7.

As another particular case, we can consider the case with $Q = 5, L = 10, N_q = 20\ \forall q$. We are located in region T_3. It is not easy to manually find the dominant configuration or to know if it is possible to saturate the condition $E_\kappa = E_\rho = 0$. In this case, using a Monte Carlo simulation, it is easy to see that it is possible to meet both conditions: each node is surrounded by others of a different colour, which in turn are different from each other. See Fig. 7 on the right. (We remark that now we are considering $q = 5$, and therefore a node can be surrounded by 4 different colours, also different from the central one).

6 Conclusion and further work

By modifying the standard Potts model with a plaquette interaction term, we have introduced a generalised model with two interaction terms, designed to yield a rich variety of mixing patterns. The model provides a flexible framework for designing collective intelligence experiments, allocating Q types of agents in a lattice. We have identified 4 different vacua regions in the phase diagram, corresponding to different arrangements, and explored how frustration manifests in some of these regions. Our findings demonstrate that by tuning the parameters κ and ρ we can control the level of homogeneity or diversity in the neighbourhood of an agent.

We want to remark that in our model implementation with M_q fixed $\forall q$, we have a different model for each choice of concrete values of M_q. Therefore from the point of view of statistical mechanics, we have a different model for each election, and then we don't have universal properties. In the model without fixed magnetization, that is to say, the standard Macrocanonical study, we expect a universal behaviour, and then critical exponents could be computed. This will be the objective of a next research, as realistically the CI experiments will always happen at finite size and do not benefit from an exact infinite volume solution.

Table 2 Parameter selection To obtain some patterns to mix agents

κ	ρ	Neighbours about me	Neighbours to each other
$\kappa = 0$	$\rho = 0$	Random	Random
$\kappa < 0$	$\rho > 0$	Different	Equal
$\kappa > 0$	$\rho > 0$	Equal	Equal
$\kappa \approx 0$	$\rho < 0$	Different	Different

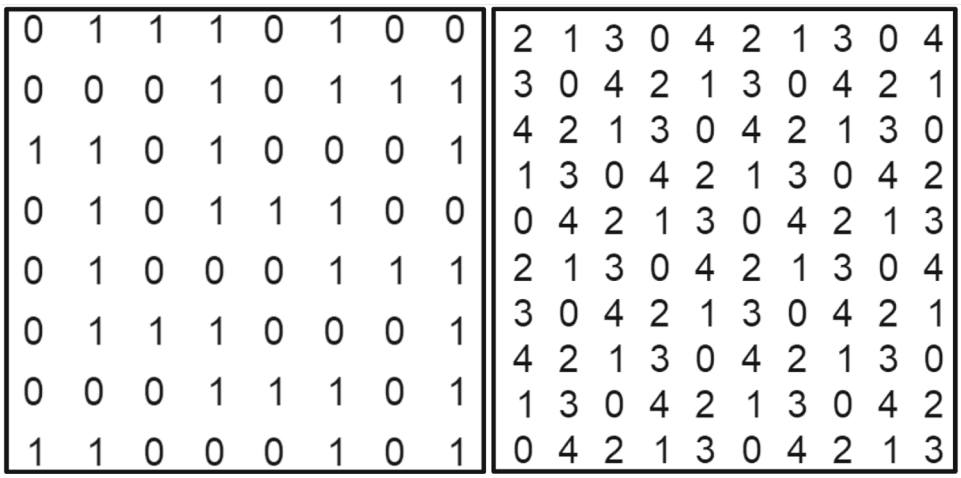

Fig. 7 Configurations in region with $\rho \ll 0, \kappa \lesssim 0$ (similar to $T3$). Left: A configuration with $Q = 2, L = 8, N_0 = N_1 = 32$. We can see a bundle with $q = 0$ around the subjacent toroidal geometry with winding number 2, and another one with winding number 1. Right: A configuration with $Q = 5, L = 10, N_q = 20\ \forall q$. In this configuration, the system is not frustrated, and we have a vacua with both energies in the minimum values $E_\rho = E_\kappa = 0$

Another topic of research will be how the different configurations, and perhaps their dynamical variation, influence the opinion propagation and thus the process of consensus.

Finally, we want to explore how the different configurations influence the mix not of human but of pure AI agents, where the strategies of [4] provide new scalable mechanisms beyond the traditional *consensus@N* or *pass@N* strategies.

Acknowledgement This work was supported in part by Grant No. PID2022-136374NB-C22, funded by the Spanish MCIN/AEI and by the European Union. We thank L. A. Fernández for useful discussions.

Author contributions

All authors contributed equally to the theoretical approach and its discussion. CT raised the initial question and supervised the solutions. AT did the Monte Carlo calculation and the main draft of the sectorial analysis. AR did the final expanded version of the manuscript, as well as the integration with the collective intelligence tool.

Funding Information Open Access funding provided thanks to the CRUE-CSIC agreement with Springer Nature.

Data Availability Statement There are no experimental data associated with the work in this paper. The data associated with the collective intelligence tool referred in the text is presented and analysed in separate papers by the users of the tool and is not directly relevant to the work presented here.

Code Availability Statement The code to generate Monte Carlo configurations is available upon request to the authors.

References

1. R. Axelrod, The dissemination of culture: a model with local convergence and global polarization. J. Confl. Resolut. **41**(2), 203–226 (1997)
2. C. Castellano, S. Fortunato, V. Loreto, Statistical physics of social dynamics. Rev. Mod. Phys. **81**(2), 591–646 (2009)
3. P. Dandekar, A. Goel, D.T. Lee, Biased assimilation, homophily, and the dynamics of polarization. Proc. Natl. Acad. Sci. U.S.A. **110**(15), 5791–5796 (2013)
4. T. García-Egea, A. Rivero, A. Tarancón, C. Tarancón, The physics of Collective Human Intelligence and opinion propagation on the lattice. Phys. Lett. A **522**, 129767 (2024)
5. N. Gradwohl, A. Strandburg-Peshkin, H. Giese, Humans strategically avoid connecting to others who agree and avert the emergence of network polarization in a coordination task. Sci. Rep. **13**, 11299 (2023)
6. S.J. Ferreira, A.D. Sokal, Antiferromagnetic Potts models on the square lattice. Phys. Rev. B **51**, 6727–6730 (1995)
7. L. Gauvin, J. Vannimenus, J.P. Nadal, Phase diagram of a Schelling segregation model. Eur. Phys. J. B **70**, 293–304 (2009)
8. M. Itakura, Mean-field analysis of antiferromagnetic three-state Potts model with next-nearest-neighbor interaction. Phys. Rev. B **55**, 48–51 (1997)
9. M. Jusup, P. Holme, K. Kanazawa et al., Soc. Phys. Phys. Rep. **948**, 1–148 (2022)
10. Y. Liu, W. Liu, X. Gu, Y. Rui, X. He, Y. Zhang, LMAgent: a large-scale multimodal agents society for multi-user simulation. arXiv:2412.09237
11. N. Lanchier, The Axelrod model for the dissemination of culture revisited. Ann. Appl. Probab. **22**(2), 860–880 (2012)
12. H. Meyer-Ortmanns, Immigration, integration and ghetto formation. Int. J. Mod. Phys. C **14**(3) (2003)
13. S. Orejudo et al., Evolutionary emergence of collective intelligence in large groups of students. Front. Psychol. **13**, 848048 (2022)
14. M. Perc, J.J. Jordan, D.G. Rand et al., Stat. Phys. Coop. Phys. Rep. **687**, 1–51 (2017)
15. T. Schelling, Dynamic models of segregation. J. Math. Sociol. **1**(2), 143–186 (1971)
16. C. Schulze, Potts-like model for Ghetto formation in multi-cultural societies. Int. J. Mod. Phys. C **16**(03), 351–355 (2005)
17. D. Stauffer, H. Meyer-Ortmanns, Simulation of consensus model of Deffuant et al on a Barabási–Albert Network. Int. J. Mod. Phys. C **15**(02), 241–246 (2004)
18. D. Stauffer, S. Solomon, Ising, Schelling and self-organising segregation. Eur. Phys. J. B **57**, 473–479 (2007)
19. A.J. Stewart, M. Mosleh, M. Diakonova et al., Information gerrymandering and undemocratic decisions. Nature **573**, 117–121 (2019)
20. A. Szolnoki, M. Perc, Competition of tolerant strategies in the spatial public goods game. New J. Phys. **18**(8), 83021 (2016)
21. M. Del Vicario, G. Vivaldo, A. Bessi et al., Echo chambers: emotional contagion and group polarization on Facebook. Sci. Rep. **6**, 37825 (2016)
22. A.W. Woolley, I. Aggarwal, *Collective Intelligence and Group Learning* (Oxford University Press, Oxford, 2020)